Localized Electron Transfer in Nonpolar Solution: Reaction of Phenols and Thiophenols with Free Solvent Radical Cations

Ortwin Brede,*,† Mahalaxmi R. Ganapathi,† Sergej Naumov,‡ Wolfgang Naumann,‡ and Ralf Hermann†

Interdisciplinary Group Time-Resolved Spectroscopy, University of Leipzig, Permoserstr. 15, D-04303 Leipzig, Germany, and Institute of Surface Modification, Permoserstr 15, D-04303 Leipzig, Germany

Received: July 27, 2000; In Final Form: January 25, 2001

Free electron transfer (FET) is understood as the reaction of free and uncorrelated solvent parent radical cations with solutes characterized by a lower ionization potential than those of the solvent. We studied electron transfer from phenols and thiophenols (as solutes) to molecular radical cations of some nonpolar solvents (cyclohexane, *n*-dodecane, 1,2-dichloroethane, *n*-butyl chloride) using pulse radiolysis. For phenols (ArOH) as solutes, along with the expected radical cations $ArOH^{\bullet+}$, an unexpectedly comparable amount of phenoxyl radicals ($ArO^{\bullet}$) was observed, which evidently arises in a parallel reaction channel of the type shown below with cyclohexane as the solvent: $c\text{-}C_6H_{12}^{\bullet+} + ArOH \rightarrow c\text{-}C_6H_{12} + ArOH]^{\bullet+}$, $ArO^{\bullet}$, H^+_{solv}. Analogous observations were also made for thiophenols as solutes, with $ArSH^{\bullet+}$ and $ArS^{\bullet}$ simultaneously occurring as reaction products. The appearance of cations and radicals as parallel products can be attributed to two alternative, locally different electron transfer pathways of FET. For example, in the case of phenol it was assumed that transfer starts from either the aromatic ring or the hydroxyl group of the solute. The occurrence of $ArO^{\bullet}$ as a reaction product can then be understood if an efficient transfer barrier prevents rapid charge equilibration in the ionized solute and, therefore, boosts deprotonation. On the basis of quantum chemical calculations, this hypothesis is proven by analyzing the molecular oscillations. From the effects observed, general conclusions about FET are derived which characterize this transfer as unhindered, extremely rapid electron jumps from the donors to the holelike solvent radical cations taking place within almost the first collision between the reactants in the solvent cage.

Introduction

Studying detailed mechanisms of electron transfer processes in organic systems is a widespread subject of reaction kinetics. Here we focus attention on ion molecule reactions of saturated molecular radical cations in nonpolar solution, which exhibit some surprising peculiarities of electron transfer dynamics.

Radical cations of organic molecules in liquid solution are often metastable and decay on a nanosecond time scale by deprotonation, fragmentation, reaction with nucleophiles, etc. This holds in particular for radical cations of saturated nonpolar liquid compounds such as alkenes and alkyl chlorides, which can be generated radiolytically, known as parent ions.[1−6]

$$RX \rightsquigarrow RX^{\bullet+} + e^-_{solv} \qquad R = \text{alkyl, } X = H, Cl \quad (1)$$

In liquids at room temperature, these species exist for a few hundred nanoseconds and have excellent electron acceptor properties owing to the high ionization potential of the ground-state molecules.

Regarding electron transfer mechanisms, the commonly known photosensitized electron transfer[7] is well-described by the Rehm−Weller kinetic scheme,[8] in which the transfer steps include the reactants' approach, the encounter complex formation, the transfer event, and ion separation[9] (cf. eq 2, where * denotes an electronically excited state):

$$A^* + D \rightleftarrows [A^*...D] \rightleftarrows [A^{\bullet-}...D^{\bullet+}] \rightleftarrows A^{\bullet-} + D^{\bullet+} \quad (2)$$

In contrast to this mechanism, the analogous equilibrium system for the reaction of the parent ions involves only one charged species in each step,[3] where S stands for the solute.

$$RX^{\bullet+} + S \rightleftarrows [RX^{\bullet+}...S] \rightleftarrows [RX...S^{\bullet+}] \rightleftarrows RX + S^{\bullet+} \quad (3)$$

From reaction 3 it is apparent that this ion−molecule reaction mechanism can be very efficient if a favorable ionization potential difference between solvent and solute leads to a reduced Franck−Condon barrier for the forward transfer step.[10] Hence for process 3, the activation barrier should be much less significant than in process 2, and may not even exist at all. For this reason, and also by virtue of the involvement of free ions,[11a] the ion−molecule reaction 3 has been defined as free electron transfer (FET).[12,13]

Using the pulse radiolysis technique,[14] FET has been utilized in the past to generate a variety of solute radical cations, e.g. refs 15−18. In a rapid process, product radical cations are formed in (3) in what is assumed to be a very selective manner. *n*-Alkanes,[2] cyclohexane,[1] dichloroethane,[5] and in particular *n*-butyl chloride[3] were found to be useful as basic solvents.

Recently, a surprising product distribution was found for FET from various phenolic compounds to solvent parent cations. Instead of exclusively phenol radical cations ($ArOH^{\bullet+}$), phenoxyl radicals ($ArO^{\bullet}$) were also observed to be produced in a comparable amount (cf. reaction 4a,b).[12,13,19,20]

† University of Leipzig.
‡ Institute of Surface Modification.

10.1021/jp002701o CCC: $20.00
Published on Web 03/28/2001

$$RX^{\bullet+} + ArOH \rightarrow ArOH^{\bullet+} + RX \quad (4a)$$

$$RX^{\bullet+} + ArOH \rightarrow ArO^{\bullet} + H^{+}_{solv}, RX \quad (4b)$$

The same phenomenon exists for aromatic thiols as electron donors, with thiophenol radical cations ($ArSH^{\bullet+}$) and thiyl radicals ($ArS^{\bullet}$) appearing as products of FET.[12,13]

It was demonstrated that the products $ArOH^{\bullet+}$ and $ArO^{\bullet}$ were actually formed by electron transfer[4] because the decay of the solvent parent ions and the formation of the two different products takes place synchronously, as was confirmed by analyzing the time profiles of all the species involved. Reaction (4) proceeds at room temperature with rate constants of about $(1-2) \times 10^{10}$ dm^3 mol^{-1} s^{-1}, which is typical of diffusion control and in this case is slightly influenced by the primarily inhomogeneous distribution of the radiation-generated parent species.[3,11b]

In this paper we briefly report the experimental details, give a detailed interpretation of the product distribution phenomenon observed in the cases of phenols and thiophenols, and comprehensively consider the consequences for free electron transfer in general.

Experimental Section

Pulse radiolysis experiments were performed with high-energy electron pulses (1 MeV, 15 ns duration) generated by a pulse transformer accelerator ELIT (Institute of Nuclear Physics, Novosibirsk, Russia). The absorbed dose per pulse measured with an electron dosimeter was between 50 and 100 Gy, corresponding to transient concentrations of around 10^{-5} mol dm^{-3}. Details of the pulse radiolysis setup are reported elsewhere.[21,27]

The solvents *n*-butyl chloride,[3] 1,2-dichloroethane,[5] cyclohexane,[1] and *n*-dodecane[4] were purified as reported. The spectrograde substances from Aldrich and Merck were generally dried using molecular sieve chromatography. The phenols and thiophenols were of maximum commercial grade (Merck) and used as received.

Phenol and thiophenol radical cations have generally been found to be much less sensitive to oxygen than radicals.[13,20] Whereas phenol samples were purged with nitrogen gas, thiophenol solutions were purged with pure oxygen; this serves the transformation of radiolytically formed reactive alkyl radicals into alkylperoxyls, which in our time range do not react with thiols.[22] Alkyl chlorides are internal scavengers for solvated electrons formed by solvent ionization. Using the alkanes as solvents, 0.1 mol dm^{-3} carbon tetrachloride was added to scavenge electrons.[23] In the nonpolar solutions, an imaginable aggregate formation of phenols and thiophenols (dimers or multimers) was ruled out by ^{1}H NMR measurement of the chemical shifts depending on the solute concentration, using ring current effects as the probe.

The kinetic fits of the superimposed transient absorption time profiles were performed using the programs ACUCHEM and ACUPLOT,[24] which numerically solve the differential equation for the assumed reaction mechanism. To adjust the concentration profiles to those of optical absorption, reasonable extinction coefficients were used which were determined independently, e.g. by one-electron oxidation in aqueous solution.[20,25]

Quantum chemical calculations were performed with the density functional theory hybrid B3LYP with 6-31G(d) basis set[26] using Gaussian 98. This enabled vibration analysis of the phenol and thiol molecules and geometry calculation of frontier orbitals.

Results

In pulse radiolysis, primarily the solvents are ionized. Then the solvent parent radical cations react with the solutes (here, e.g., ArOH) according to reaction 5.

$$RX^{\bullet+} + ArOH \rightarrow RX + \text{products } (ArOH^{\bullet+}, ArO^{\bullet}) \quad (5)$$

As mentioned in the introduction, all the electron transfer reactions involving the different phenols or thiophenols showed a uniform diffusion-controlled rate constant, which was governed only by the solvent viscosity. In our case, all the rate constants formally determined from the decay of the solvent radical cation signals in the presence of solutes are $k_{4,5} = (1-2) \times 10^{10}$ dm^3 mol^{-1} s^{-1}, because of the similar viscosities of the solvents used[13,19,20] (not documented here). The same rate constant values were also observed using the deuterated phenol 4-Cl−Ar−OD. Hence, typical scavenger concentrations for taking product transient spectra are $\geq 2 \times 10^{-3}$ mol dm^{-3}. Taking this and diffusion control of reaction 5, after about 30 ns the reaction is almost complete. Using 15 ns pulses, the spectrum of the products can be taken shortly after the pulse.

Although sometimes mentioned elsewhere under the aspect of radical cation identification and decay kinetics,[12,13,27] we demonstrate and discuss in detail three prominent examples of localized free electron transfer[4] from a phenol, a thiophenol and 4-hydroxythiophenol to parent radical cations of different nonpolar solvents.

Phenol in 1,2-Dichloroethane Solution. Pulsing a solution of 10^{-2} mol dm^{-3} phenol in 1,2-dichloroethane, electron transfer (5) proceeds rapidly, and the product spectrum of the phenol transients can be seen immediately after the 15 ns pulse (cf. Figure 1). The transient spectrum shows three maxima at wavelengths around 300, 400, and 440 nm. The spectral gap around 280 nm is caused by the depletion of the parent phenol. Upon adding 0.1 mol dm^{-3} ethanol, the 440 nm absorption is completely quenched, whereas the remaining absorption is markedly reduced compared to the ethanol-free sample. This absorption fits those well-known for the phenoxyl radical[28] ($ArO^{\bullet}$). The absorption peaking at 440 nm is classified as being caused by the phenol radical cation ($ArOH^{\bullet+}$); see also ref 19. The situation explaining the spectral behavior of Figure 1 can be described by electron transfer[4] synchronously forming $ArOH^{\bullet+}$ and $ArO^{\bullet}$. The quenching effect of ethanol acts in two modes, deprotonating the radical cation (reaction 6) and competing with electron transfer[4] by deprotonating the parent cation (reaction 7)

$$ArOH^{\bullet+} + C_2H_5OH \rightarrow ArO^{\bullet} + C_2H_5OH_2^{+} \quad (6)$$

$$ClCH_2CH_2Cl]^{\bullet+} + C_2H_5OH \rightarrow ClCH_2C^{\bullet}HCl + C_2H_5OH_2^{+} \quad (7)$$

Looking at the time profiles given in Figure 1b,c, at 400 nm a longer lasting species and at 430 nm a short-living transient can be distinguished, corresponding well to our interpretation of the transient types $ArO^{\bullet}$ and $ArOH^{\bullet+}$. Certainly, the two time profiles represent superimpositions of both transients, with one dominating.

Whereas the deactivation of phenoxyl radicals (reaction 8) is comparably slow, the phenol radical cation decays

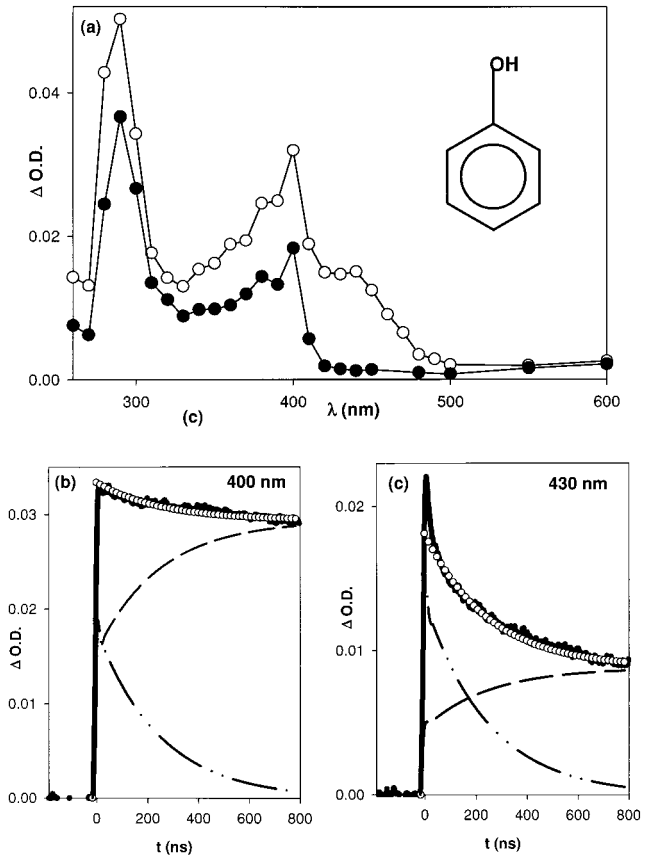

Figure 1. (a) Transient optical absorption spectra of a N_2-bubbled solution of 10^{-2} mol dm^{-3} phenol in 1,2-dichloroethane taken 30 ns after the electron pulse (○). After adding 0.1 mol dm^{-3} ethanol (●), the cation part is quenched. (b, c) Transient time profiles at $\lambda = 400$ and 430 nm taken from the original sample (bold line). The fit curves describe the decay of $ArOH^{\bullet+}$ (— • •) and the $ArO^{\bullet}$ kinetics (— —) consisting in a rapid (4a) and delayed (9) part as well as the sum fit (○).

markedly by a first-order process explained by deprotonation[2] (reaction 9).

$$2ArO^{\bullet} \rightarrow \text{products} \qquad 2k_8 = 3 \times 10^8\ \text{dm}^{-3}\ \text{mol}^{-1}\ \text{s}^{-1} \quad (8)$$

$$ArOH^{\bullet+} \rightarrow ArO^{\bullet} + H^+_{solv} \qquad k_9 = 3 \times 10^7\ \text{s}^{-1} \quad (9)$$

We then fitted the time profiles numerically using reasonable kinetic and spectroscopic parameters (parent cation generation within the pulse followed by product formation with k_4; for the fate of the species using k_8 and k_9, fitting the time profiles with the experimental ratio of the extinction coefficients). The kinetic behavior of $ArOH^{\bullet+}$ and $ArO^{\bullet}$ is described by the following differential equations:

$$d[ArOH^{\bullet+}]/dt = k_{4a}[ArOH][RX^{\bullet+}] - k_9[ArOH^{\bullet+}]$$

$$d[ArO^{\bullet}]/dt = k_{4b}[RX^{\bullet+}][ArOH] + k_9[ArOH^{\bullet+}] - k_8[ArO^{\bullet}]^2$$

Figure 1b,c shows two examples of fits performed at various wavelengths (400 and 430 nm) using the same rate constants and only varying ϵ values. The nonfitted spike (430 nm) is explained by residual solvent cation absorption. Apart from this, the fits excellently describe the decay of $ArOH^{\bullet+}$ as well as the fast (due to reaction 4b) and delayed formation (due to reaction 9) of $ArO^{\bullet}$.

TABLE 1: Ratio of the Products of the Electron Transfer (4) Evaluated from the Fit Operation for Different Solvents

phenol, ArOH	$k_9 \times 10^6$ [s^{-1}], $ArOH^{\bullet+}$ deprotonation	ratio $[ArOH^{\bullet+}]/[ArO^{\bullet}]$ in FET (4a,b)	solvent generating $RX^{\bullet+}$
phenol	1.9	1.00	c-C_6H_{12}
	2.8	0.92	*n*-$C_{12}H_{26}$
	3.5	1.00	*n*-C_4H_9Cl
	3.5	0.92	1,2-$C_2H_4Cl_2$
4-Cl-	3.0	1.00	c-C_6H_{12}
	3.1	0.92	*n*-$C_{12}H_{26}$
	3.1	1.04	*n*-C_4H_9Cl
	3.4	1.00	1,2-$C_2H_4Cl_2$
4-Cl-Ar-OD	3.0	1.02	*n*-C_4H_9Cl
4-MeO-	3.1	1.00	*n*-$C_{12}H_{26}$
	2.9	0.92	*n*-C_4H_9Cl
	3.0	1.04	1,2-$C_2H_4Cl_2$
4-Me-2,6-di-*t*-Bu-	1.8	1.12	c-C_6H_{12}
	3.7	1.00	*n*-$C_{12}H_{26}$
	2.1	1.00	*n*-C_4H_9Cl
	2.9	1.00	1,2-$C_2H_4Cl_2$
4-NH_3-	0.9		*n*-C_4H_9Cl
4-NO_2-	4.0		*n*-C_4H_9Cl
n-octadecyl (3,5-di-*t*-Bu-4-OH-phenyl)propionate	2.0	1.13	*n*-C_4H_9Cl
4-MeO-thiophenol, ArSH	4.5	0.82	c-C_6H_{12}
	4.8	0.75	*n*-$C_{12}H_{26}$
	4.8	0.82	*n*-C_4H_9Cl
	3.2	0.85	1,2-$C_2H_4Cl_2$

Because the delayed formation[9] of the phenoxyl radicals is directly proportional to the decay of the phenol radical cations, we have a quantitative measure of the relation between the two reaction channels of the FET[4] divided into the formation of $ArOH^{\bullet+}$ (4a) and $ArO^{\bullet}$ (4b). In the example given, the portions are nearly the same; i.e., both species are formed with the same probability expressed by the ratio $[ArOH^{\bullet+}]/[ArO^{\bullet}]$. This seems to be irrespective of the solvent used (cf. Figure 1) and amounts for phenol to an average of 0.96. Analogous experiments, data evaluation, and fits were performed with various substituted phenols in different solvents, with nearly identical results showing transient ratios around 1. All the resulting parameters are given in Table 1. Only in the case of a sterically hindered phenol with a very long tail in the 4-position did the transient ratio of 1.13 indicate a larger amount of $ArOH^{\bullet+}$.

***p*-Methoxythiophenol in Cyclohexane.** As already mentioned, thiophenols exhibit analogous effects in free electron transfer (4), with the radical cations $ArSH^{\bullet+}$ and $ArS^{\bullet}$ also being formed in comparable amounts. The kinetic and spectral parameters of the two transient types have already been listed for many thiophenols in a former paper.[13] Here we demonstrate and analyze the situation of FET with respect to the transient ratio using the new example of *p*-methoxythiophenol dissolved in cyclohexane. Figure 2 gives the transient absorption spectra of a solution of 10^{-2} mol dm^{-3} of the thiol in cyclohexane taken immediately after the electron pulse. Three absorption bands can be distinguished at $\lambda = 320$, 520, and 580 nm. The latter is short-lived and identified by the ethanol reaction analogous to reaction 9 caused by the thiophenol radical cation. The other two bands can predominantly be explained by the thiyl radical. Representative time profiles are shown in parts b (510 nm) and c (570 nm) of Figure 2. To save space, suffice it to state that data analysis was performed in exactly the same manner as described above for phenol. The time profile at $\lambda = 570$ nm shows the kinetic behavior of *p*-MeO−Ar−$SH]^{\bullet+}$ with good separation. The transient superimposition was fitted with

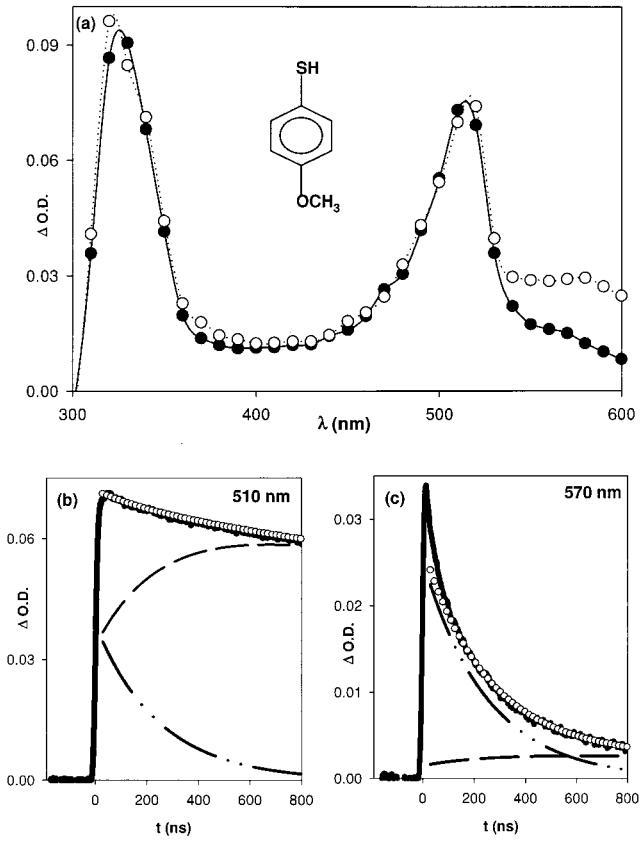

Figure 2. (a) Transient optical absorption spectra of an O_2 bubbled solution of 10^{-2} mol dm^{-3} 4-methoxythiophenol in cyclohexane containing 0.1 mol dm^{-3} carbon tetrachloride (○, taken after 30 ns). After adding 0.1 mol dm^{-3} ethanol (●, taken 30 ns after the pulse), the cation part is quenched. (b, c) Transient time profiles at $\lambda = 510$ and 570 nm taken from the original sample (bold line). The fit curves describe the decay of $ArSH^{\bullet+}$ (– ••) and the $ArS^{\bullet}$ kinetics (– –) consisting in a rapid (4a) and delayed (9) part as well as the sum fit (○). The profile in panel c describes nearly pure $ArSH^{\bullet+}$ kinetics.

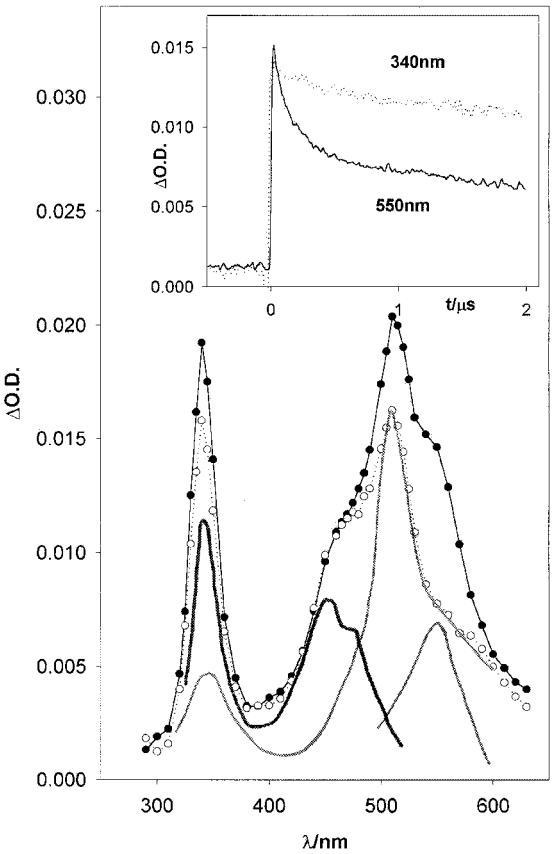

Figure 3. Transient optical absorption spectra of an O_2-bubbled solution of 10^{-2} mol dm^{-3} 4-hydroxythiophenol in *n*-butyl chloride taken immediately after the electron pulse (●) and after 1.5 μs (○). The unmarked spectra are calculated by adjusting the known spectrum[12] of HO−Ar−S$^{\bullet}$ at the 520 nm peak of the spectrum (○). Taking differences, the spectrum of $^{\bullet}$OH−Ar−SH (bold faced, λ_{max}= 350 and 450 nm) and of HO−Ar−SH$]^{\bullet+}$ (λ_{max} = 550 nm) result.

experimental parameters for radical recombination (10) and radical cation deprotonation (11).

$$2ArS^{\bullet} \rightarrow \text{products} \qquad 2k_{10} = 3.5 \times 10^{9}\ \text{dm}^3\ \text{mol}^{-1}\ \text{s}^{-1} \tag{10}$$

$$ArSH^{\bullet+} \rightarrow ArS^{\bullet} + H^{+}_{solv} \quad k_{11} = 5 \times 10^{6}\ \text{s}^{-1} \tag{11}$$

In this example of free electron transfer analogous to reaction 4, the relation between the channels seems to be shifted toward the formation of $ArS^{\bullet}$ (55%) instead of $ArSH^{\bullet+}$ (45%), expressed by a ratio value of 0.81. For many thiophenols studied, the FET phenomenon with two synchronous reaction channels (5a,b) has also been reported[13].

FET Involving 4-Hydroxythiophenol Dissolved in *n*-Butyl Chloride. When studying encounter geometry control of product distribution in free electron transfer (4), the question arises as to how benzene rings with more than one OH or SH group behave. For this purpose we studied 4-hydroxythiophenol (10^{-2} mol dm^{-3}) in *n*-butyl chloride solution. Figure 3 shows absorption spectra of this sample taken immediately after the 15 ns electron pulse and after 1.5 μs, from which the radical cation absorption can be taken as a difference spectrum showing the absorption of HO−Ar−SH$]^{\bullet+}$ peaking at 550 nm. This part can be completely quenched by a small amount of ethanol as elucidated above for the other product cations. With the known spectrum of HO−Ar−S$^{\bullet}$ (ref 12) adjusted at the 520 nm peak after 1.5 μs (also shown in Figure 3), it can easily be seen that a further radical transient is hidden in the sum absorption. Taking the difference spectrum of this, only a typical phenoxyl radical absorption spectrum appears. This clearly indicates the formation of three different products formed in parallel in the FET and formulated in eq 12, where for simplicity's sake the proton removed from the polar groups is not shown.

$$\text{OH−Ar−SH} + \textit{n}\text{-}C_4H_9Cl^{\bullet+} \rightarrow \text{OH−Ar−SH}]^{\bullet+}, {}^{\bullet}\text{O−Ar−SH}, \text{OH−Ar−S}^{\bullet} + n\text{-}C_4H_9Cl \tag{12}$$

These results convincingly show the product control of the reactants' encounter geometry. Because of the strong superimpositions of the species (also seen in the inset of Figure 3 from time profiles), we were unable to quantitatively analyze the effect in the same way as described above. However, speculating with extinction coefficients of similar radicals and radical cations it can be assumed that the three channels (corresponding to the three products) participate to about the same extent in the FET, with the radical cation channel forming OH−Ar−SH$]^{\bullet+}$ possibly being of minor importance.

Discussion

Overall, the phenomenon of the encounter-controlled product distribution in free electron transfer from phenolic and/or thiophenolic molecules to parent ions of nonpolar solvents has

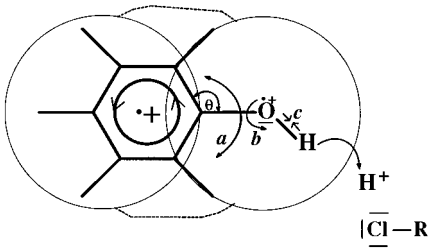

Figure 4. Schematic illustration of the dynamics of the phenol molecule involved in free electron transfer (4).

been clearly established by several experimental examples, which can also be extended to larger aromatic ring systems such as substituted naphthalenes and biphenyls.[13,20] Below we interpret the phenomenon in more detail.

Analysis of the Electron Transfer Reaction Steps. Considering the individual steps of the electron transfer according to the equilibrium system,[3] the reactants approach by molecular diffusion, which is the slowest process in the sequence and, therefore, rate-determining. Consequently, the FET as the gross reaction also exhibits rate constants of diffusion control. This involves any time-resolved measurements being limited to the nanosecond time scale and being quasi-stationary with respect to the higher rate of the other FET steps. However, the pulse radiolysis experiments clearly rule out other conceivable formation paths for the phenol transients, such as normal radical reactions or formation via electronically excited states.

If the parent ions and the solute meet by diffusion, different sterical configurations ought to be possible in the encounter position. Therefore, if not sterically excluded, electron transfer from the solute to the solvent ion should be possible from both the aromatic ring and the hydroxyl group. Hence FET takes place in nearly every reactant approach, producing parallel phenol radical cations and a local cation center in the hydroxyl group. At least two types of encounter situations should occur, as symbolized in the eq 13 reaction sequence of FET from phenol to *n*-butyl chloride radical cations.

Clearly, distinguishing between the two transfer product formation channels as given in reactions 13 only makes sense if there is a bottleneck between the aromatic ring and the hydroxyl group impeding rapid internal electron equilibration after the electron transfer step. Hence the deprotonation of Ar−O$^{\bullet+}$H is favored, rather than its stabilization by charge distribution.

This interpretation can theoretically be assisted by analyzing the dynamics of the phenol molecule in ultrashort times (cf. Figure 4). The phenol molecule is surrounded by an ellipsoid symbolizing the encounter region. This ellipsoid is arbitrarily divided into two subspheres each describing the range of highest probability of local electron transfer, at either the aromatic ring or the hydroxyl group. This electron transfer is suggested to be an extremely rapid electron jump, proceeding in each encounter geometry immediately or after just a few collisions. This is assumed due to the different local ionization potentials, which are higher for the hydroxyl than the aromatic group. If several encounters were needed for successful electron transfer, the highest enthalpy difference ought to control the process; however, this is contrary to all the experimental observations. Within the encounter zone, the reactants form something like a supermolecule, existing only in the momentum of the electron transfer, which should take place in the subfemtosecond time range. This is also the time range in which charge equilibration should take place throughout the aromatic moiety (broken line area).

Assuming this to be the case, it is unclear why the electron jump at the hydroxyl group does not also undergo the rapid charge equilibration. Here we hypothesize that a distinctly short-lived steric barrier exists. Analysis of the dynamics of molecular oscillations and in particular of the bonds around the oxygen reaction center reveals the relatively slow deformation motion of the bond from the aromatic C-atom to the phenolic oxygen (a) (cf. Figure 4). Furthermore, there is a very extended rotation motion of the OH group along the C−O axis (b). Both oscillations happen in times of ≥100 fs, making them very slow compared with intramolecular electron exchange. The above-mentioned intramolecular oscillations upset the geometry favorable for intramolecular electron exchange until about 100 fs. Whereas (a) brings the OH group out of the aromatic plane, (b) changes the HOMO orbital interaction of the nonbinding constellation at the C−O bond dramatically. Statistically speaking, only after about 100 fs is a geometry achieved in which charge equilibration can efficiently succeed. Table 2 summarizes the molecular dynamic data as frequencies and times of one motion.

Compared to this, the vibration motion of the O−H bond (c) is at least 30 times faster than the above-mentioned fluctuating electron exchange barrier caused by deformation and rotation motions (a and b). c brings about additional polarization of the bond, and so the proton can be set free. Additionally, the escape of H^+ is promoted by the nucleophilic and solvation properties of the solvent.

Concerning the orbital symmetries, the C−O bond MO, which results from the negative or out-of-phase combination of two atomic orbitals, is of an antibonding character and has a node (value of zero) between the atoms. That the electronic coupling really changes during the rotation of the OH group around the C−O axis can be seen from orbital symmetries. Considering the Klopman−Salem equation[28,29] for describing the interaction energy of two molecules in the ground state, we used the coefficients for atomic orbital interaction $C_{c,o}$ to assess the intramolecular electron exchange situation between the OH group and the aromatic ring, in particular concerning the O−C barrier. This was calculated for situations in which the OH group is twisted out of plane by 30°, 60°, or 90°. Then the quantum chemically calculated C_o and C_c values of the orbitals change by decreasing the overlap between AOs (bonding character), which is well-expressed by the product of the squares of the *C*-values [$C_o^2 \times C_c^2$]. Hence, when using normalized values, a change from 1.00 (0°), 0.84 (30°), 0.35 (60°), to 0.26 (90°) results. This clearly indicates that the electronic coupling element of the molecular electron exchange varies considerably with the twist of the OH along the C−O axis.

Taking the electron equilibration as intramolecular electron transfer, the electronic coupling matrix element strongly influences the transfer rate by modulating the transfer probability depending on the angle of twist of the OH group. On an

$$\mathrm{Ar{-}OH} + \mathrm{C_4H_9Cl^{\bullet+}} \begin{cases} \rightarrow [\mathrm{HO{-}Ar...^{\bullet+}C_4H_9Cl}] \rightarrow [\mathrm{Ar^{\bullet+}OH...C_4H_9Cl}] \rightarrow \mathrm{ArOH]^{\bullet+} + C_4H_9Cl} \\ \rightarrow [\mathrm{Ar{-}OH...^{+\bullet}C_4H_9Cl}] \rightarrow [\mathrm{Ar{-}O^{\bullet+}H...C_4H_9Cl}] \rightarrow \mathrm{ArO^{\bullet} + H^+(ClC_4H_9)} \end{cases} \quad (13)$$

TABLE 2: DFT B3LYP/6-31G(d) Calculated Frequency Analysis of the Molecular Oscillations around the Polar Group XH in Phenol and Thiophenol[a]

		ArOH		ArSH	
motions	locality	$\nu \times 10^{12}$ (Hz)	t (fs)	$\nu \times 10^{12}$ (Hz)	t (fs)
deformation 1	C−XH	7.0	143	5.5	182
deformation 2	C--XH	23.3	43	14.4	69
rotation of OH	C--XH	10.8	92	3.5	285
vibration	C--X--H	112.4	8.9	81.3	12.3

[a] Deformation of the polar group within the aromatic plane: 3.9°(ArOH), 3.3°(ArSH). Times (t) are those of one motion.

electronic basis, this provides a strong argument for the existence of the above-mentioned fluctuating barrier for the intramolecular electron exchange.

Considering the vibration dynamics of molecules, isotope labeling enables the frequencies of the various molecular modes to be influenced. Concerning the C−O bond, instead of labeling O^{18}-H, substituting oxygen by sulfur as in thiolphenols should be considered. Here, the heavy sulfur reduces the frequencies of a and b, and the vibration mode c also lasts a bit longer. Table 2 compares the discussed molecular motions for phenol and thiophenol. And indeed, the transient product ratio observed after FET (4) is different in this path (4b) with rapid $ArS^{\bullet}$ formation seeming to dominate (cf. Figure 1). Speculating about the reason, the larger volume of the sulfur group could be responsible for this effect. Also in this case, the different solvents used do not affect the product ratio.

Labeling the phenolic hydrogen by substituting with deuterium does not bring about an effect different from that of normal phenol, neither for the electron transfer rate k_4 nor for the product distribution. This was studied in detail for 4-chlorophenol and is documented in Table 1. Then again, this result is not surprising because the O−D vibration is not expected to differ dramatically from that of O−H, calculated to be 1.4 times slower.

Hence for phenols and thiols of different electronic structure, the identical effect in the free electron transfer reaction (5) is observed—the synchronous formation of both metastable radical cations and stable heteroatom localized radicals. The independence of the molecule electronics can be understood in terms of the rapid, free electron transfer, which is only governed by the geometry of collisions. The same reason seems to hold also for the case of the long-chain substituted phenol, where the remaining C_{18} might have an antenna function, increasing the yield of $ArOH^{\bullet+}$.

Concerning reaction (4b), such processes are often considered as normal one-step deprotonation reactions. In this case, however, we are convinced that an extremely fast electron transfer (within about 10^{-15} s) is taking place, followed by a delayed fast deprotonation driven by the O−H vibration oscillation (around 10^{-13} s); otherwise, for simple deprotonation, an influence of the electronic structure of the molecules would be expected. Therefore in this particular case of the phenols and thiols, the principal reaction paths of electron transfer (4a) and electron transfer with slightly delayed deprotonation (4b) can be distinguished, whereas simple deprotonation (cf. 9) in this system takes much longer. On the basis of our experiments, we can also rule out an imaginable hydrogen atom transfer (14),

$$RX^{\bullet+} + HO-Ar \rightarrow [RXH^{\bullet+}...HO-Ar] \rightarrow RXH^{+} + ArO^{\bullet} \quad (14)$$

which could compete with reaction 4a instead of reaction 4b. Such a hydrogen transfer should show a kinetic isotope effect for OD labeling, which was not found to be the case (see above). Furthermore, in distinction to the electron transfer processes (4a,b) discussed in this paper, H atom transfer (14) should proceed mostly activation-controlled via a defined encounter state (see also the subsequent paragraphs).

General Consequences for the FET Mechanism. Whereas in radiation chemistry the nonrelaxed solvent radical cations (holes) have been the subject of much attention by virtue of their extreme mobility (up to 100 times faster than molecular ions[31−34]), electron transfer reactions of the relaxed molecular parent radical cations have been less thoroughly investigated. Concerning holes, the existence of such unusually mobile species seems to be a general phenomenon in the radiation-induced ionization of saturated hydrocarbons,[33b] largely influenced by the actual structure of the alkanes, especially alicycles such as cyclohexane[31a−c] and decaline,[31d] which have a longer lifetime. The high mobility of holes is also reflected by free electron transfer[31a,33a] with its extremely high rate constants.

$$[c\text{-}C_6H_{12}]^{\bullet+}* + S \rightarrow c\text{-}C_6H_{12} + S^{\bullet+}$$
$$k_{14} = 10^{12}\ dm^3\ mol^{-1}\ s^{-1}\ (ref\ 33a) \quad (15)$$

where the asterisk denotes a molecule in the hole state

Ignoring the question over the mechanism of hole motion, the high rate values of reaction 15 indicate that the electron transfer step in FET is very rapid, and the approach of the reactants by diffusion or other forms of motion is generally the rate-determining step of FET.

Returning to the subject of this paper, pulse radiolysis studies in the 1970s showed that molecular and relaxed radical cations of alkanes ($\geq C_6$), of C_6 alicycles such as cyclohexanes, and of alkyl chlorides are metastable up to 200 ns in liquids and at room temperature and, therefore, can be used for FET[10,35] (4). In accordance with plausibility considerations and also with low-temperature EPR measurements,[35a] quantum chemical calculations show that in the parent ions the charge is distributed throughout the entire saturated molecules,[35b] certainly partially influenced by the actual molecular structure. Seen as a defect electron in an exclusive σ bond system, the term "hole" also has some justification for the molecular parent ion.

As such holelike species in condensed systems are the subject of this investigation, it is no surprise that these parent radical cations normally react in a diffusion controlled manner in the free electron transfer assumed to be a function of the reaction-enthalpy difference between the partners expressed, e.g., by the ionization potential difference.[10] Compared with other molecular electron transfers in liquids such as the well-known photosensitized process (2), FET exhibits a number of peculiarities as listed below.

(1) FET only takes place in nonpolar solvents where the parent radical cations are metastable for kinetically reasonable times (between 10 and 200 ns). In our experience acetone is the solvent with the highest polarity which can still be applied,[15,17] characterized by dielectric constant ($\epsilon = 20.56$) and dipolar moment ($\mu = 2.70$), but best defined by Reichart's solvent polarity parameter[36] $E_T^N = 0.355$. By the way, phenol radical cations generated in acetone exhibit a lifetime of a few nanoseconds.

(2) Because of the low polarity of the solvents, the majority of the excess energy of the FET step ought to be dispersed by molecule oscillation modes of the reactants. The solvent reorganization energy is only of very minor importance.[9] Therefore, years ago we explained the dispersion of $-\Delta G$ by the excitation of different reactant molecule vibrations.[10] This model well explains the energetic relations in FET.

(3) As typical of most electron transfer types, the change to the electronic state in the transfer step is rapid compared with the time necessary for nuclear rearrangements in the reactant molecules. But as already mentioned, the time of the electron jump in FET is a few orders of magnitude faster than sensitized processes (2), the encounter state of which was recently characterized in a time-resolved manner[37] using femtosecond spectroscopy.

(4) Regarding the rapid electron jump in FET suggested to be comparable with the rate of intramolecular electron exchange in aromatic systems proceeding in times roughly estimated to lie around 10^{-15} s, the term encounter complex becomes more formal and evolves into a question of philosophy in reaction dynamics. We consider the electron jumps to comprise an adiabatic transition in an electronically strongly coupled system. The term "encounter complex" hence takes on the meaning of a supermolecule formed by the reactants in which the electron transition is practically unhindered. Assuming such a supermolecule, the interaction of the reactants ("collisions") are relative motions of the partners in ultrashort times. Hence, the electron jump can really take place in the subfemtosecond time range. However, we are aware that this point is highly critical and should be the subject of further theoretical investigation.

In the Introduction, the formulation used of the individual steps of the free electron transfer as a system of equilibria (3) should be also reconsidered. As we stated, FET is the energetically favored filling of a positive hole (parent ion), and such a process has very limited reversibility. After electron transfer (5), the former parent ion becomes part of the weak solvation shell of the product cation and enters something like an anonymous situation. The memory of the former reaction partner is therefore lost. The inherent properties of free electron transfer discussed in this paragraph justify considering this reaction type as a very distinct version of the commonly known electron transfer processes. Here it should be mentioned that this effect could be also considered as two steps in a resolved special case of dissociative proton coupled electron transfer theoretically treated by Cukier.[38]

Conclusions

Pulse radiolysis experiments on the free electron transfer from phenols to solvent parent radical cations of alkanes and alkyl chlorides resulted in the surprising observation that, in addition to the expected product radical cations, phenoxyl radicals were also formed to a comparable extent. We explain this phenomenon by local electron jumps involving both molecule functions as the aromatic ring and the hydroxyl group. Whereas in the first case the charge is immediately equilibrated throughout the aromatic moiety (subfemtosecond range), the ionized hydroxyl group exists locally for up to 100 fs due to a slowly fluctuating reaction barrier in the form of deformation and rotation oscillations. Hence the kinetically dominating process is deprotonation at the positively charged heteroatom group rather than charge equilibration. This deprotonation is assumed to proceed in the time range of the vibration oscillation of the O−H bond, which is faster than the fluctuating barrier.

This phenomenon was observed for many phenols and thiophenols as well as hydroxyl- and thiyl-substituted naphthalenes and biphenyls, showing that the reported observations are due to a general effect of electron donors such as aromatics substituted with OH and SH groups, which are rather unstable in ionized form. Hence, even for double-substituted aromatics such as 4-hydroxythiophenol (HO−Ar−SH), local energy transfer in a modified form was demonstrated, leading in this case to three distinct products. Such localized electron jumps are assumed to also occur for all other scavenger molecules, but in most cases they cannot be detected. This is generally a distinct feature of electron transfer reactions, which to the best of our knowledge is unknown in this localized form precisely for such small molecules (such phenols) in solution. Up till now, similar local electron transfer effects were observed only from aromatic donor groups separated by more or less rigid saturated hydrocarbon bridge spacers (e.g. by 10 σ bonds corresponding to 12 Å) to solvent ions.[39−41]

From the detailed studies reported in this paper, some general conclusions can be drawn about the mechanism of free electron transfer. Courageously, it should be stated that transfer as a real electron jump takes place extremely rapidly in the subfemtosecond time range, as generally unhindered electron motion is understood to proceed. Because of the holelike nature of the parent ions, the electron jump proceeds adiabatically in an electronically strongly coupled supermolecule of the reactants. This calls for common equilibrium considerations with encounter and successor complexes as intermediates. In this sense, this paper presents new information on electron transfer dynamics in the condensed phase.

References and Notes

(1) Mehnert, R.; Brede, O.; Bös, J. *Z. Chem. (Leipzig)* **1977**, *17*, 268.
(2) Brede, O.; Mehnert, R., Naumann, W.; Cserep, Gy. *Radiat. Phys. Chem.* **1982**, *20*, 155.
(3) Mehnert, R.; Brede, O.; Naumann, W. *Ber. Bunsen-Ges. Phys. Chem.* **1982**, *86*, 525.
(4) Mehnert, R.; Brede, O.; Naumann, W. *Ber. Bunsen-Ges. Phys. Chem.* **1984**, *88*, 71.
(5) Shank, N. E.; Dorfman, L. M. *J. Chem. Phys.* **1970**, *52*, 4441.
(6) Le Motais, B. C.; Jonah, C. D. *Radiat. Phys. Chem.* **1989**, *33*, 505.
(7) Marcus, R. A. *Annu. Rev. Phys. Chem.* **1964**, *15*, 155 and subsequent papers.
(8) Rehm, D.; Weller, A. *Ber. Bunsen-Ges. Phys. Chem.* **1969**, *73*, 834.
(9) Survey in: Kavarnos, G. J. *Fundamentals of Photoinduced Electron Transfer*, VCH Publ.: New York, 1993; pp 287.
(10) Brede, O.; Mehnert, R.; Naumann, W. *Chem. Phys.* **1987**, *115*, 279.
(11) (a) Busi, F. In *The Study of Fast Processes and Transient Species by Electron Pulse Radiolysis;*. Baxendale, J. H., Busi, F., D., Eds.; Reidel Publ. Comp.: Dordrecht, 1982; pp 418−421. (b) Hummel, A. In *Radiation Chemistry, Principles and Application;* Fartahaziz, Rodgers, M. A. J., Eds.; VCH Publ.: Weinheim, 1987; pp 98−135.
(12) Dey, G. R.; Hermann, R.; Naumov, S.; Brede, O. *Chem. Phys. Lett.* **1999**, *310*, 137.
(13) Hermann, R.; Dey, G. R.; Naumov, S.; Brede, O. *Phys. Chem. Chem. Phys.* **2000**, *2*, 1213.
(14) Sauer, M. C.; Fielden, E. M.; Roffi, G. in *The Study of Fast Processes and Transient Species by Electron Pulse Radiolysis*, Eds. Baxendale, J. H.; Busi, F., D. Reidel Publ. Comp.: Dordrecht, 1982. pp 35−89.
(15) Rodgers, M. A. J. *J. Chem. Soc., Faraday 1* **1973**, *68*, 1278, 2036.
(16) Brede, O.; Bös, J.; Helmstreit, W.; Mehnert, R. *Radiat. Phys. Chem.* **1982**, *19*, 1.
(17) Lomoth, R.; Naumov, S.; Brede, O. *J. Phys. Chem. A* **1999**, *103*, 2641.
(18) Guldi, D. M.; Asmus, K.-D. *J. Am. Chem. Soc.* **1997**, *119*, 5744.
(19) Brede, O.; Orthner, H.; Zubarev, V.; Hermann, R. *J. Phys. Chem.* **1996**, *100*, 7097.
(20) Mohan, H.; Hermann, R.; Naumov, S.; Mittal, J. P.; Brede, O. *J. Phys. Chem. A*, **1998**, *102*, 5754.
(21) Brede, O.; David, F.; Steenken, S. *J. Chem. Soc., Perkin Trans. 2* **1995**, *2*, 23.
(22) Schöneich, C.; Dillinger, U.; von Bruchhausen, F.; Asmus, K.-D. *Arch. Biochem. Biophys.* **1992**, *292*, 456.
(23) Mehnert, R.; Brede, O.; Naumann, W. *J. Radioanal. Nucl. Chem.* **1986**, *101*, 307.
(24) Braun, W.; Herron, J. T.; Kahaner, D. K. *Int. J. Chem. Kinet.* **1988**, *20*, 51.
(25) Alfassi, Z. B.; Schuler, R. H. *J. Phys. Chem.* **1985**, *89*, 3359.
(26) Becke, A. D. *J. Chem. Phys.* **1993**, *98*, 5648; Becke, A. D. *J. Chem. Phys.* **1996**, *104*, 1040.
(27) Mahalaxmi, G. R.; Hermann, R.; Brede, O. *Phys. Chem. Chem. Phys.* **2000**, *2*, 4947.

(28) Land, E. J.; Porter, G. *J. Chem. Soc. Trans. Faraday Soc.* **1966**, *59*, 2027.
(29) Klopman, G. *J. Am. Chem. Soc.* **1968**, *90*, 223.
(30) Salem, L. *J. Am. Chem. Soc.* **1968**, *90*, 543, 553.
(31) (a) Zador, E.; Warman, J. M.; Hummel, A. *Chem. Phys. Lett.* **1973**, *23*, 363; (b) de Haas, M. P.; Warman, J. M.; Infelta, P. P.; Hummel, A. *Chem. Phys. Lett.* **1975,** *31*, 382. (c) Warman, J. M.; Infelta, P. P.; de Haas, M. P.; Hummel, A. *Chem. Phys. Lett.* **1976**, *43*, 321. (d) de Haas, M. P.; Hummel, A.; Infelta, P. P.; Warman, J. M. *Can. J. Chem.* **1977**, *55*, 2249.
(32) Beck, G.; Thomas, J. K. *J. Phys. Chem.* **1972**, *76*, 3856.
(33) (a) Brede, O.; Helmstreit, W.; Mehnert, R. *Chem. Phys. Lett.* **1974**, *28*, 43; (b) Brede, O.; Bös, J.; Naumann, W.; Mehnert, R. *Radiochem. Radioanal. Lett.* **1978**, *35*, 85.
(34) Review: Trifunac, A. D.; Sauer, M. C., Jr.; Shkrob, I. A.; Werst, D. W. *Acta Chem. Scand.* **1997**, *51*, 158.
(35) (a) Lindgren, M., Shiotani, M. In *Radical Ionic Systems—Properties in Condensed Phases;* Lund, A., Shiotani, M., Eds.; Kluwer Academic Publ.: Dordrecht, 1991; pp 125 (b) Mehnert, R. In *Radical Ionic Systems—Properties in Condensed Phases* Lund, A., Shiotani, M., Eds.; Kluwer Academic Publ.; Dordrecht, 1991; p 231.
(36) Reichardt, C. *Solvents and Solvent Effects in Organic Chemistry*; VCH: New York, 1990.
(37) Zhong, D.; Bernhardt, T. M.; Zewail, A. H. *J. Phys. Chem. A* **1999**, *103*, 10093.
(38) Cukier, R. I. *J. Phys. Chem. A* **1999**, 5989
(39) Closs, G. L.; Miller, J. R. *Science* **1988**, *240*, 440.
(40) Johnson, M. D.; Miller, J. R.; Green, N. S.; Closs, G. L. *J. Phys. Chem.* **1989**, *93*, 440.
(41) Warman, J. M.; Hom, M.; Paddon-Row: M. N.; Oliver, A. M.; Kroon, J. *Chem. Phys. Lett.* **1990**, *172*, 114.